Mutual influence of locality and chaotic dynamics on quantum controllability

S. Kallush[1] and R. Kosloff[2]
[1]*Department of Physics, ORT-Braude College, P.O. Box 78, Karmiel IL-21982, Israel*
[2]*The Institute of Chemistry, Hebrew University, Jerusalem IL-91904, Israel*
(Received 29 April 2012; published 23 July 2012)

Quantum control tasks are classified either as classical-like or as quantum requiring interference of pathways. We study the generation of interference pathways and relate them to the fidelity of the control target at a fixed time for various tasks. The model drift Hamiltonian studied is the two-dimensional Henon-Heiles (HH) potential. This system shows regular classical dynamics for low energies and chaotic dynamics for higher energies. A control operator supported by the whole momentum space and therefore connecting the entire Hilbert phase space is a random spiky potential. The other extreme is a smooth control potential. Intermediate cases are obtained by filtering the random spiky potential in momentum space. The fidelity of achieving a control task was related to the connectivity in phase space of the control operators. Typical quantum tasks such as generating a superposition of generalized coherent states rely on interfering pathways. For these cases the nonlinearity in the drift or control Hamiltonian is a necessary requirement for creating interferences. Control over rapidly diverging components of the wave function is achieved by the use of highly nonlocal control operators. Quantum control under chaotic drift was found to give a better yield than control under regular dynamics for such cases. For classical tasks we study the transformation of an initial generalized coherent state to another one. The best fidelity is obtained for regular or harmonic regions of the potential and smooth control operators. The approach to the classical limit is checked by decreasing the effective value of $\hbar$. Control under both quantum and classical tasks suffered from the decrease of $\hbar$ and the approach to classical proximity. Classical control tasks which rely heavily on maintaining a generalized coherent state throughout the evolution were found to be dysfunctional and lead to a completely uncontrolled situation once the classical chaos starts to appear.

DOI: 10.1103/PhysRevA.86.013420 PACS number(s): 32.80.Qk, 05.45.Mt, 02.30.Yy, 03.67.−a

I. INTRODUCTION

Quantum control (QC) is dedicated to steering a quantum objective from an initial state to a final target. The basic ingredient for QC is to utilize multiple interfering pathways of the dynamics to achieve a desired goal [1,2]. Is there a control field that can achieve a desired result?

A. Control problem: The control, the drift, and the relation to controllability

Controllability of quantum systems deals with an existence principle. This issue has been addressed in an algebraic formulation [3–5]. A generic control Hamiltonian takes the form

$$\hat{\mathbf{H}} = \hat{\mathbf{H}}_0 + \sum_j \alpha_j(t)\hat{\mathbf{A}}_j, \tag{1}$$

where $\hat{\mathbf{H}}_0$ is the free drift Hamiltonian, $\alpha_j(t)$ are the control fields, and the set $\{\hat{\mathbf{A}}\}$ forms a closed control Lie algebra of operators. A closed quantum system is completely controllable provided the commutators generated by the control operators with the uncontrolled Hamiltonian $\hat{\mathbf{H}}_0$ generate the trivial algebra $\hat{\mathbf{U}}(N)$ that includes all the available Hilbert space. The existence of a possible control does not give a clue how to actually find such a control field. The task of obtaining a control field is termed the inversion problem. This paper will try to investigate the role of the various components of a control problem, that is, the drift, the control, and the types of control tasks (see below) on the ability to achieve the inversion.

B. Classification of control tasks

Optimal control theory (OCT) has been developed to find a control field to achieve a quantum objective subject to constraints [6–9]. The task of finding such a field is nonlinear since the control field alters dynamically the Hamiltonian of the systems. As a result, iterative procedures have been developed to find the control field. The number of iterations required to converge to a control field of high fidelity vary vastly reaching a number that can scale exponentially with the Hilbert space size [8,10]. Once the control field is found, could it be utilized for the same objective with the same control Hamiltonian in a larger Hilbert space?

Previously we were able to connect the computation complexity of obtaining a high fidelity control field to the algebraic structure of the control problem [10]. State-to-state control tasks can be classified by two categories with respect to the generalized coherent states (GCS) of the control algebra. GCS are defined as quantum states with maximum purity or minimum uncertainty with respect to the control algebra [11].

(1) Easy control tasks: GCS to GCS. For these control tasks a control field found for a system of a small scale can serve as pilot fields to generate solutions for larger systems efficiently. The dynamics of such processes follows a continuous set of GCSs. This can be interpreted by dynamics characterized via a single classical path, independent of the size of the systems Hilbert space.

(2) Difficult control tasks: These targets can be characterized as generating superpositions of GCSs, for example, merging a superposition of two GCSs to a single one. Such objectives require a control field where the intermediate states are supported by a vast part of the Hilbert space. In addition,

the control field is not scalable, meaning that a unique field is required for each Hilbert space size.

These categories also apply to the influence of the unavoidable noise generated by the control fields $\alpha(t)$. For difficult control tasks upon increasing the size of Hilbert space the noise will dominate, destroying some of the control tasks resulting in a loss of complete controllability [12].

The classification of a control task to quantum requiring interference and classical-like has been suggested recently using different criteria [13]. The idea is to employ the one- vs two-photon control scenario as a classification tool. These criteria rely on the fact that single-photon processes are insensitive to phase control. Quantum control tasks are ones that are phase sensitive and are generated by multiple photon transition. The two approaches have a common goal to differentiate a control task dominated by interference from ones that the control field is employed to modify an effective potential on which a single control trajectory resides. The classical control task should therefore be insensitive to a change in the effective $\hbar$ for the same control Hamiltonian. The classification criteria employed here are based on the fact that the control that achieves a classical path is nearly invariant to a change in Hilbert space, maintaining the inner structure of the classical Hamiltonian. This fits the time domain control approach used throughout this study.

Recently, Moore *et al.* [14] have classified the computational difficulty of obtaining a control field. They defined the depth of a control operator $\hat{\mathbf{A}}$ as the number of commutations with $\hat{\mathbf{H}}_0$ that generate a state-to-state connection. They found that for low-depth control Hamiltonians the task becomes more difficult with the increase in the size of the system. In this case the control operators do not connect the whole Hilbert space directly. On the other hand, for high-depth control operators that connect directly distant states of $\hat{\mathbf{H}}_0$, the difficulty of the task changes only slightly with size.

C. Mutual influence of the drift, the control, and the environment

In this paper, the two notions of classicality of the dynamics and locality of the control operators will be combined to asses the contribution of multiple path interferences in the control. To do so, quantum control tasks will be examined in the presence of classically regular and chaotic drift Hamiltonians. The basic conjecture is that quantum control requiring multiple paths will prefer chaotic dynamics which maximize interferences, while a single-path scalable control task will be preferably obtained under regular conditions.

We remark hereby that the quantum systems that will be used in this paper are such that their classical analog of the drift Hamiltonian $\hat{\mathbf{H}}_0$ is chaotic. By decreasing $\hbar$ for the same $\hat{\mathbf{H}}_0$ we increase the effective Hilbert space size and approach the classical limit. The pure quantum dynamics under the drift Hamiltonian is regular since the quantum-mechanical evolution of a closed quantum system is quasiperiodic [15]. Considering that searching for the control field is a nonlinear process, could the underlying classically chaotic Hamiltonian affect the generation of a state-to-state control task?

This paper is arranged as follows. In the next section the formal model for the uncontrolled and controlled Hamiltonians will be presented. Section III will present the role of chaos on the invertibility and discuss the result of operator localization, and Sec. IV will add conclusive remarks.

II. FORMAL MODEL

For the drift generator of the dynamics, a Hamiltonian $\hat{\mathbf{H}}_0$ is studied which is classically chaotic and tunable. The Henon-Heiles (HH) Hamiltonian (with the mass taken as 1) was chosen as our two-dimensional model system [16]

$$\begin{aligned}\hat{\mathbf{H}}_0 &= \frac{1}{2}\left(\hat{\mathbf{P}}_x^2+\hat{\mathbf{P}}_y^2\right)+\hat{\mathbf{V}}(x,y),\\ \hat{\mathbf{V}}(x,y) &= \frac{x^2+y^2}{2}+\lambda(x^2y-y^3/3).\end{aligned} \tag{2}$$

For $\lambda = 0$, the potential is harmonic, the system is separable and decomposed into normal modes. As a result, the classical dynamics are regular. For the localized control set $\{\hat{\mathbf{A}}_{\rm loc}\} \equiv \{\hat{\mathbf{P}}_x,\hat{\mathbf{P}}_y,\hat{\mathbf{X}},\hat{\mathbf{Y}}\}$, the generalized coherent states (GCSs) of this system are products of coherent states in the x and y coordinates $|\alpha_x\rangle \otimes |\alpha_y\rangle$. These states are the most classical-like with respect to the position-momentum phase space. The set $\{\hat{\mathbf{A}}_{\rm loc}\}$ with the drift Hamiltonain Eq. (2) is completely controllable if the dissociation channels of the HH potential are blocked. For $\lambda = 0$ the set is not completely controllable; for example, there is no control field which can split an initially localized GCS into a superposition of GCSs.

For nonzero λ, the potential is nearly harmonic close to the origin $\{x,y\} = \{0,0\}$. As a result, the spectrum at low energies is similar to a two-mode harmonic spectrum. For energies that are closer to the dissociation limit of the potential $E \leqslant 1/6\lambda^2$, anharmonicity becomes dominant. In this regime the classical motion is chaotic showing the signatures of chaos such as a finite Kolmogorov entropy [15,17] and positive Lyapunov exponent. For a closed quantum system the dynamics are regular, however, the onset of chaos will appear as a rapid spreading of an initial localized wave packet [18,19]. Throughout this paper we choose $\lambda = 0.11108$. For this value of λ, about half of the bound spectrum of the HH potential is in the classically chaotic region, where well-pronounced chaotic dynamics are obtained with small islands of stability.

The consequence of quantum scars [20] in the chaotic dynamics of the HH model are shown in Fig. 1. A GCS chosen by the localized control algebra is displaced by Δ on the x direction and is propagated under $\hat{\mathbf{H}}_0$. Under this displacement, the energy is determined by the harmonic term as $E = \Delta^2/2 + 1$. The temporal generalized purity is a measure of the projection of the wave function on the subspace of GCSs. In this case the GCSs are localized phase-space functions which are the product of harmonic oscillator coherent states in x and y. The temporal generalized purity is a measure of the projection of the wave function on the subspace of GCSs. In terms of the generalized purity a wave funtion that is projected into a single GCS is a (generally) pure state with minimal uncertainty and maximal resemblance to classical distribution. A reduction of the generalized purity is thus a sign for an increased uncertainty and a nonclassical wave function. We have to remark here that the generalized purity is not to be confused with the conventional purity of quantum states, which is defined by the trace of the square of the density matrix,

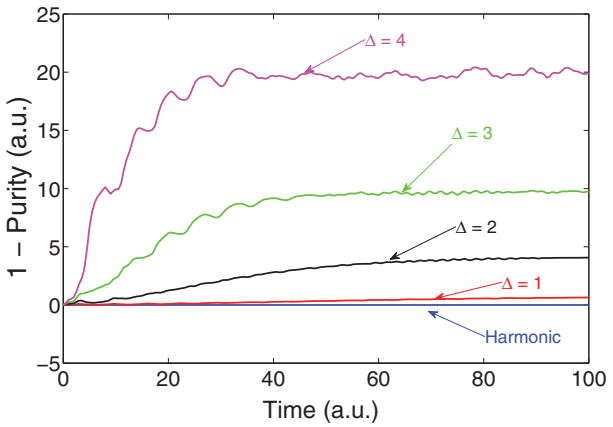

FIG. 1. (Color online) Signatures of chaotic dynamics generated by the HH potential. The temporal purity of the system as a function of time for harmonic and HH potentials. Different initially localized CS displaced by Δ with respect to the origin are shown.

so that a variation of this purity will take place only under non-Hamiltonian dynamics. From here on, we use solely the term purity to denote generalized purity.

The purity can be related to the uncertainty with respect to the localized control algebra

$$1 - \mathcal{P} = \Delta\hat{\mathbf{x}} + \Delta\hat{\mathbf{p}}_x + \Delta\hat{\mathbf{y}} + \Delta\hat{\mathbf{p}}_y, \tag{3}$$

where $\Delta\hat{\mathbf{A}} \equiv \langle\hat{\mathbf{A}}^2 - \langle\hat{\mathbf{A}}\rangle^2\rangle^{\frac{1}{2}}$ is the uncertainty of the operator $\hat{\mathbf{A}}$. This generalized purity is a measure of the spread of the wave function over phase space. As can be seen in the figure, a localized GCS with minimal purity remains GCS under a harmonic Hamiltonian and for relatively low energies ($E = 2$ for $\Delta = 1$) also under the HH potential. For higher energies, in the HH case the state spreads rapidly over the whole available phase space and the purity decreases until it saturates once the whole phase space is covered. In what follows the physical unit of time is the harmonic period (2π). The total target time for control is chosen as $T = 100$. This time is much longer than the harmonic period of the system. However, this time is much shorter than the recurrence time scale of this system.

The set of local phase-space controls $\{\hat{\mathbf{A}}_{\rm loc}\}$ connects directly only a small band of states in the drift Hamiltonian $\hat{\mathbf{H}}_0$. We seek a control operators set $\{\hat{\mathbf{A}}\}$, with higher connectivity. This set has to be nonlocal with respect to coherent states in phase space. We choose control operators $\hat{\mathbf{A}}_j(x,y)$ diagonal or local in position space so that they do not couple directly different position in the phase space. The nondiagonal or nonlocal coupling of such a potential-like operator is at the momentum space. The nonlocality in the momentum representation depends on the roughness of the control operator in position. For smooth functions, for example, a typical dipole coupling operator ($\hat{\mathbf{A}} \propto \hat{\mathbf{X}}$), the momentum nonlocality is very limited. The operator is semilocal also in momentum. To obtain a nonlocal momentum control operator, we choose a random matrix in position, with zero averaged energy. For unbiased comparison the integrated energy of the control operator $\iint A_j^2 dxdy$ was kept normalized to unity. Localization of the control operators was obtained by applying a Gaussian filter in momentum space. This was done by a forward two-dimensional (2D) discrete Fourier transform leading to $\tilde{\mathbf{A}}_\mathbf{j}(\mathbf{p_x},\mathbf{p_y})$. Then the operators are multiplied by the function

$$F(p) = \exp\left(-p^2/\sigma L_p^2\right), \tag{4}$$

where L_p is the extent of the grid in momentum space and σ is the width of the filtering window in fractions of the total momentum grid. The grid size employed in this study was 64×64, and in position the grid extent used is $L_R = 12$ bohr, so that $L_p = N\hbar/L_R = 5\frac{1}{3}$ of momentum units. Figure 2 plots an example for the localization of the potential with the decrease of the filtering width. The reduction of high momentum components leads to smoothing of the control function, which is quantified by the autocorrelation function.

The relation between the control operators, the control task, and the final fitness for a fixed target time will be examined in the next section. To account for the randomness of the control operator, each given data point is averaged over ten different realizations. The averaged fitness values are calculated for each value of the parameters. The standard deviations are denoted by error bars. Convergence tests were performed to ensure the consistency of the procedure. The number of realizations was doubled for some of the data points, verifying that the results are indeed converged.

The control tasks were carried out using local control (LC) [21–23] for a fixed time interval. The method is unidirectional and ensures a monotonic increase of the fitness with time. The instantaneous control field(s) is (are) obtained by the expression

$$\alpha_j(t) \propto -\mathrm{Im}\langle\hat{\mathbf{P}}\hat{\mathbf{A}}_j\rangle_{\psi(t)}, \tag{5}$$

where $\hat{\mathbf{P}}$ is the projection operator into the given target state. The expectation values are calculated with respect to the instantaneous wave function $\psi(t)$. Six random operators $\hat{\mathbf{A}}_j$ were used for each realization. A global optimal-control-theory-based algorithm was applied with the localized control as an initial pilot field. With a small number of iterations the fitness only slightly improved. Significant improvement by OCT demands a significantly larger computation effort, and thus was omitted. Note, however, that the use of LCT does not imply a weak field control, and, as will be demonstrated below, during the control the amplitude moves back and forth between the various states extensively.

III. RESULTS

A. Control with nonlocal operators

Control tasks employing nonlocal control operators are studied first. The target is to transform a displaced CS into the ground state, also a CS. To reduce the differences between the chaotic and regular drift Hamiltonians, the initial state was displaced only on the x axis, where the anharmonicity of the potential vanishes [see Eq. (2)]. According to our definition in Ref. [10] this kind of task could be classified as classical-like, that is, a transition that could be executed without interferences. However, as will be presented below, for nonlocal operators which couple the whole phase space this advantage is not exploited. Figure 3 shows the deviation from maximal fitness at the final time, for different initial displacements Δ. The solid red and dashed blue lines refer to drift dynamics

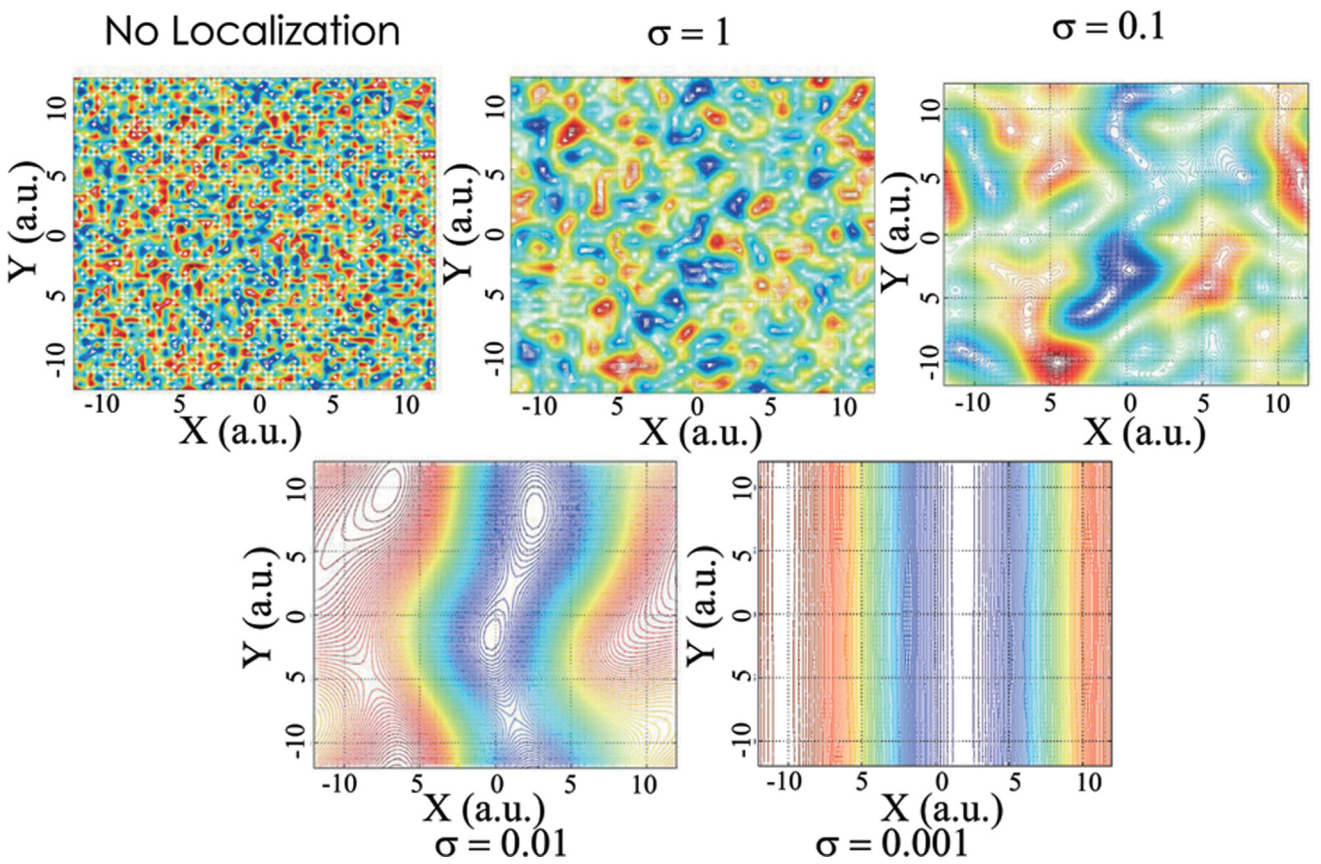

FIG. 2. (Color online) Localization of the control potential matrices. Example for a single realization of $\hat{\mathbf{A}}(x,y)$ under Gaussian filtration. Values of the filtering parameter σ are assigned below the panels. The amplitude of the control function is kept constant throughout the filtration process. σ is in atomic units of momentum.

under regular and chaotic drift Hamiltonians, respectively. The initial state energy is given by $E = 1 + \Delta^2/2$, so that for $\Delta > 3.5$ $E > 7$, and the uncontrolled dynamics are chaotic. As can be seen from the curves, higher fitness is attainable under chaotic dynamics, and the difference increases with the increase of the initial state energy, where the chaotic character is enhanced. One should note that for very low initial state energy, where the dynamics are highly regular and the initial state almost perfectly overlaps the target, the harmonic dynamics yield better results (see inset).

To understand the mechanism of the process, several typical single realization examples for the purity vs time are shown in Fig. 4. In all cases, the solid lines refer to the dynamics under chaos and the dashed lines to regular dynamics. The initial displacement is assigned to each of the curves. For all cases, the purity which measures the spread of the wave function in phase space begins with a minimal spread that characterizes the CS. At early times, the control and the drift shuffle the system remotely from a single CS to a superposition state with low purity values. Then the control dynamics proceeds by a rearrangement step which localized back the wave function into a coherent ground state with a minimal spread. It is notable, however, that both nonlocal operators and chaotic dynamics contribute to the mechanism of the two steps (i.e, the shuffling and the rearrangement). Under regular dynamics both steps are less efficient, thus in spite of low purity at intermediate times under regular drift dynamics, the final inefficient rearrangement step results in an inferior approach to the target. Note that for extremely low initial energies the purity remains high along the trajectory. As a result, the harmonic potential achieves higher fidelity than the HH. Very similar results were obtained for quantum tasks, that is, transformations that demand interferences by construction, such as the merging of two CSs into the single ground CS. Nonlocal operators encompass the ability to create and control the spreading of the wave function. In this case the dynamics evolves through many states and low generalized purity, so that the difference between classical and quantum tasks is insignificant.

B. Local control operators

In this study, the control operators were filtered and localized in momentum space (σ was taken as 0.05). The achievement measure of the control (i.e., the fidelity) was calculated for classical tasks. Examining Fig. 5 shows the opposite behavior of the nonlocal control dynamics. Regular dynamics lead to better fitness. Control under HH potential becomes inefficient with the onset of chaos, while the increase of energy is almost insignificant for control tasks in the harmonic regime. This phenomenon is expected since there is a closed form solution for the control function in the harmonic task.

An examination of the temporal purity shows that the mechanism of the control process is to follow closely a CS

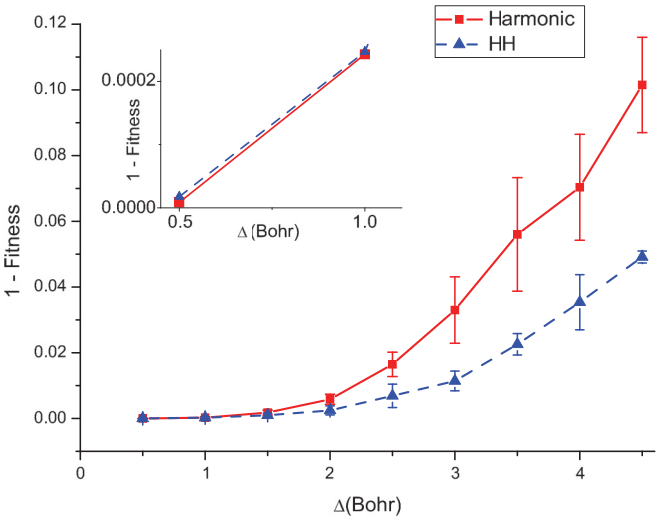

FIG. 3. (Color online) Control with nonlocal operators. The control task is the transformation of a displaced CS to the ground state. Deviation from unity of fitness vs the displacement of the initial CS. Solid red lines represent dynamics under harmonic potentials and dashed blue lines the HH potential. Inset: Data of the first two points in larger scale. The trend is inverted for these values. Results were obtained by averaging over ten realizations. Standard deviations are denoted by the error bars.

thus maintaining a high purity value. This enables the limited localized operators to control the system. Under increasingly growing chaos in the system such a mechanism ceases to operate. Note also the increase of the variance of the fitness for higher initial energies. This could be explained by the fact that the difference between poorly featured control operators could be very large, leading to large deviations between different realizations.

Figure 6 shows the fitness for the quantum task of merging a superposition of two CSs into the ground state. For such tasks interferences are necessary, and the localized operators could not achieve the control targets. The actual deviations from the target are larger by more than an order of magnitude

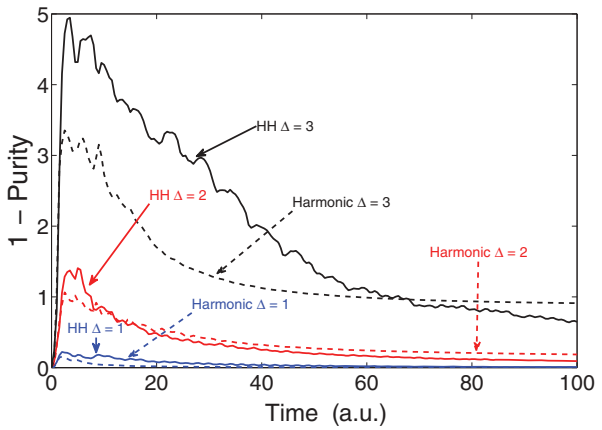

FIG. 4. (Color online) Control with nonlocal operators: Mechanism. Typical single-realization examples for the instantaneous purity vs time for different initially displaced CS and drift Hamiltonians. The conditions for each of the curves are assigned explicitly.

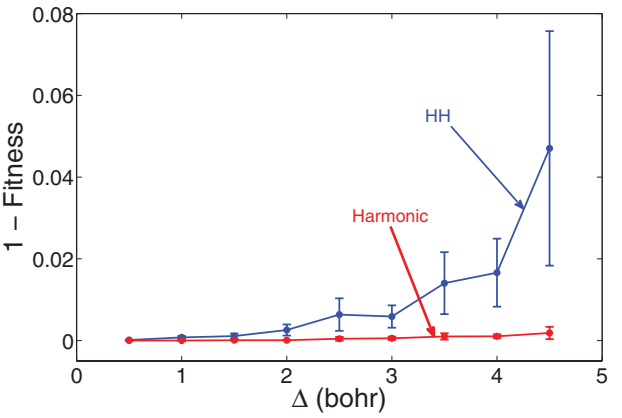

FIG. 5. (Color online) Control with localized operators: Classical tasks. Same as Fig. 3. The control operators are Gaussian filtered with $\sigma = 0.05$.

compared to the values obtained by nonlocal control operators. The necessity for interferences favors the chaotic dynamics to the regular one even for this case of poor controllability. Note, however, that in these cases the fidelity has a large variance depending on different random operator realization. As a result, the determination of the points in this graph is therefore inaccurate, and the nonmonotonic behavior of the fidelity as a function of Δ should be attributed to this artifact rather then to real physical mechanism.

C. Localization of control operator

The ability to control depends on the localization parameter. This aspect is examined in the current subsection. Figure 7 displays the deviation from maximum fitness vs the localization parameter σ for classical-like tasks. The red and black lines represent results under the harmonic oscillators drift Hamiltonian with different initial displacements, while the blue and green lines are for the chaotic drift Hamiltonian. As can be seen from the curves, under regular dynamics the localization improves the ability to control classical tasks, while under chaotic conditions there is almost no influence of the localization on the ability to control.

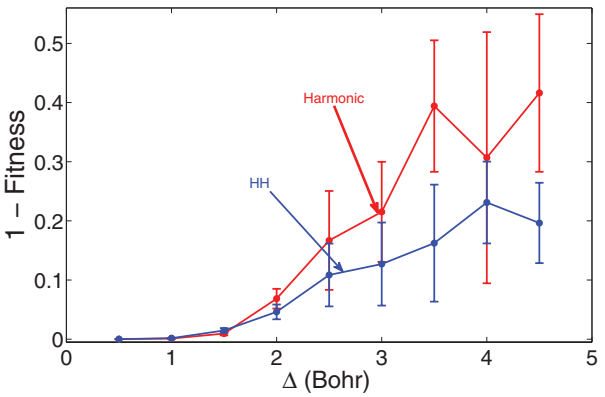

FIG. 6. (Color online) Control with localized operators: Quantum tasks. Same as Fig. 5. The control task is to merge two displaced coherent states into the ground state.

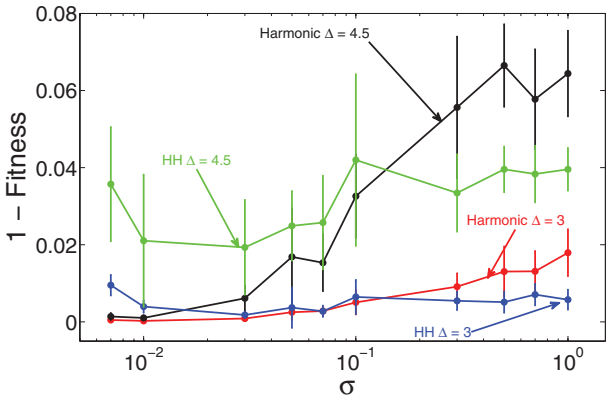

FIG. 7. (Color online) Localization: Classical tasks. Deviation of unity of fitness for the task of taking a displaced CS to the ground state vs the locality of the control operators. Displacements and drifts are assigned in the legend. σ is the operators smoothing parameter parametrized in units of parts of the momentum grid length (see details in the text).

Similarly to the previous sections, the regular dynamics exceeds the chaotic dynamics for localized control operators. The trend is inverted around $\sigma = 0.1$. Figure 8 shows the same quantities, now for the quantum task of converting a cat state into the ground state. For this case there is a monotonic decrease of the controllability for more local control operators, in all cases. Note, however, that chaotic and regular drift Hamiltonians have opposing fitness characteristics. This is obtained for lower values of σ, as the contribution of the nonlocality of the operators and the drift are more crucial than in classical tasks.

D. Approach to the classical limit

Quantum interference is responsible for the control of the difficult tasks of generating superpositions of CS. Enhanced controllability was found in the previous section to be associated with classical chaotic systems. This is in contrast to classical intuition where chaos is associated with reduced control. To study the approach of the quantum dynamics that were demonstrated at the previous sections to the classical limit, the control Hamiltonian is maintained, but the effective value of Plank's constant is varied from $\hbar$ finite to the classical limit $\hbar \to 0$. Figure 9 presents the deviation from perfect fitness vs $\hbar$, for a different localization of the control operators. The task in this example is the classical task of translating a displaced coherent state with $\Delta = 3$ back to the ground state. As can be seen from the figure, for nonlocalized control operators ($\sigma = 1$) the controllability is reduced with decreasing $\hbar$. Some residual controllability is maintained due to the pathways generated by the nonlocality.

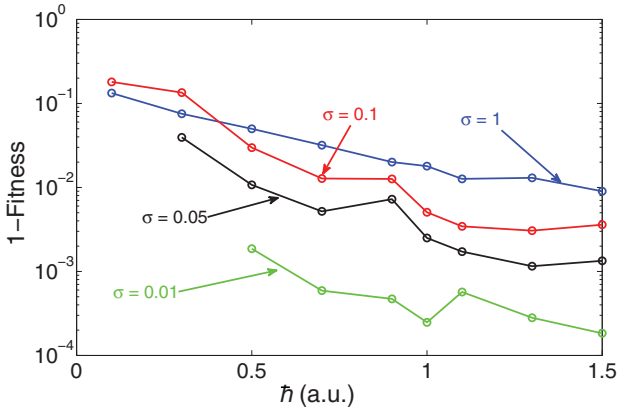

FIG. 9. (Color online) The onset of classical chaos: Classical tasks. Deviation from unity of fitness for the task of translating a displaced CS to the ground state vs $\hbar$. Displacement is set to $\Delta = 3$. The rest of the parameters are as in Fig. 7. The various curves refer to different values of localization of the control operators. Missing data points for $\sigma = 0.01$ and $\sigma = 0.05$ indicates practically zero fitness of the control task.

For the localized control operators, there is a very rapid degradation of the ability to control with the approach of the onset of classical chaos. The lack of data points for the curves for $\sigma = 0.05$ and $\sigma = 0.01$ is due to the fact that no control could be achieved. We can interpret this finding as a quantum manifestation of a transition to classical chaos, which leads to loss of controllability.

Figure 10 exhibits the deviation from perfect fitness as a function of the locality of the control operators for a quantum task of driving a symmetric superposition of coherent states

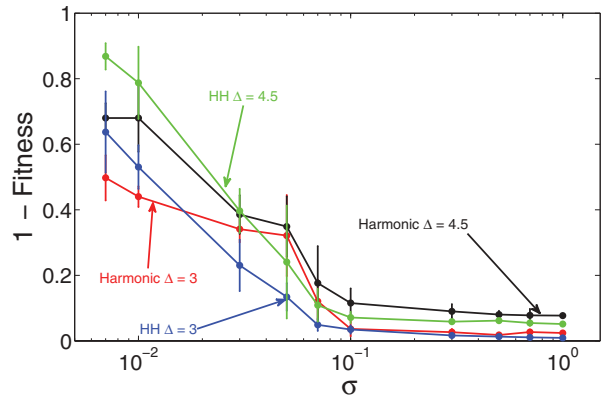

FIG. 8. (Color online) Localization: Quantum tasks. Same as Fig. 7, now for the task of taking two coherent states to the ground state.

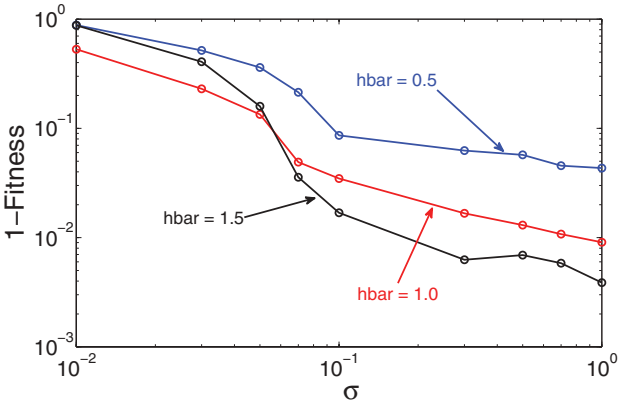

FIG. 10. (Color online) The onset of classical chaos: Quantum tasks. Deviation from unity of fitness for the task of merging two displaced CS to the ground state vs the locality parameter σ.

with $\Delta = 3$ to the ground state. Three curves for three values of $\hbar$ are shown. For quantum tasks interferences are required by construction and a decrease of control is obtained for the decrease of the locality parameter. As expected, for nonlocal operators ($\sigma \to 1$), an increase of $\hbar$ leads to better control, which results from both the increase of the quantum character of the dynamics and the reduction of the number of states. For localized control operators the inability to control interferences leads to the opposite trend, that larger values of $\hbar$ lead to poor control despite the decrease in the number of states in the Hilbert space.

IV. CONCLUSION AND FUTURE OUTLOOK

A control task depends on three components: the drift, the control, and the classical or quantum character of the task. The character of the task determines the extent of the interferences required to achieve the desired transformation. The form of the drift Hamiltonian governs the rate of the uncontrolled spread of the wave function, which leads to interferences. The form of the control operator(s) regulate the possible rate of rearrangement of the system that leads it to the goal. For quantum control tasks the environment and control operators that generate superpositions of the GCS interference are highly required. A comprehensive mix of nonlocal control operators and a drift Hamiltonian that produces sufficient disorder is necessary. Classical-like task of GCS to GCS are best obtained by localized control operators and regular drift Hamiltonians. These classical-like tasks do not require significant interferences.

Within quantum control dynamics, classical single path or multiple quantum interfering paths could be handled adequately. However, the onset of classical chaos means that control trajectories that maintain high purity along the path cannot be found. Under these conditions, even a minor deviation from high purity drives the system into uncontrollable disorder, and the inability to perform classical tasks sharply depends on the parameters. The degradation of quantum control quality under the same conditions is also monotonic but continuous.

An additional consideration is decoherence, which is generated either by noise in the controls and/or from the environment. Intuitively, and probably in the most general cases, additional noise serves mainly as a limiting agent on the ability to control. In some cases, however, like cooling and one-photon control, decoherence is strictly a necessity by which the control is attainable. A future study will try to map the relations between noise and the fundamental factors that were considered in the present study.

ACKNOWLEDGMENTS

We gratefully acknowledge financial support from the Israel Science Foundation. The Fritz Haber Center is supported by the Minerva Gesellschaft für die Forschung GmbH München, Germany.

[1] P. W. Brumer and M. Shapiro, *Principles of the Quantum Control of Molecular Processes* (Wiley-Interscience, New York, 2003).
[2] S. A. Rice and M. Zhao, *Optical Control of Molecular Dynamics* (John Wiley & Sons, New York, 2000).
[3] J. Clark and T. Tarn, J. Math. Phys. **24**, 2608 (1983).
[4] C. Lan, Q. Chi, T. Tarn, and J. Clark, J. Math. Phys. **45**, 052102 (2005).
[5] V. Ramakrishna and H. Rabitz, J. Math. Phys. **54**, 1715 (1996).
[6] S. Shi and H. Rabitz, J. Chem. Phys. **95**, 1487 (1991).
[7] R. Kosloff, S. A. Rice, P. Gaspard, S. Tersigni, and D. J. Tannor, Chem. Phys. **139**, 201 (1989).
[8] J. P. Palao and R. Kosloff, Phys. Rev. A **68**, 062308 (2003).
[9] D. J. Tannor, *Introduction to Quantum Mechanics: A Time-Dependent Perspective* (University Science Book, Sausilito, CA, 2007).
[10] S. Kallush and R. Kosloff, Phys. Rev. A **83**, 063412 (2011).
[11] A. Perelomov, *Generalized Coherent States and Their Applications* (Springer, Berlin, 1985).
[12] M. Khasin and R. Kosloff, Phys. Rev. Lett. **106**, 123002 (2011).
[13] M. Spanner, I. Franco, and P. Brumer, Phys. Rev. A **80**, 053402 (2009).
[14] K. W. Moore, R. Chakrabarti, G. Riviello, and H. Rabitz, Phys. Rev. A **83**, 012326 (2011).
[15] R. Kosloff and S. A. Rice, J. Chem. Phys. **74**, 1340 (1980).
[16] M. Henon and C. Heiles, Astron. J. **69**, 73 (1964).
[17] A. Kolmogorov, Dokl. Akad. Nauk. SSSR **124**, 774 (1959).
[18] E. J. Heller and E. B. Stechel, Chem. Phys. Lett. **90**, 484 (1982).
[19] N. Moiseyev and A. Peres, J. Chem. Phys. **79**, 5945 (1983).
[20] L. Kaplan and E. J. Heller, Ann. Phys. (NY) **264**, 171 (1998).
[21] R. Kosloff, A. D. Hammerich, and D. Tannor, Phys. Rev. Lett. **69**, 2172 (1992).
[22] R. S. Judson and H. Rabitz, Phys. Rev. Lett. **68**, 1500 (1992).
[23] V. Engel, C. Meier, and D. J. Tannor, in *Advances in Chemical Physics*, Vol. 141, edited by S. A. Rice, (John Wiley and Sons, Hoboken, NJ, 2009).